REPORT DOCUMENTATION PAGE			Form Approved OMB No. 0704-0188

Public reporting burden for this collection of information is estimated to average 1 hour per response, including the time for reviewing instructions, searching existing data sources, gathering and maintaining the data needed, and completing and reviewing the collection of information. Send comments regarding this burden estimate or any other aspect of this collection of information, including suggestions for reducing this burden to Washington Headquarters Services, Directorate for Information Operations and Reports, 1215 Jefferson Davis Highway, Suite 1204, Arlington, VA 22202-4302, and to the Office of Management and Budget, Paperwork Reduction Project (0704-0188), Washington, DC 20503.

1. AGENCY USE ONLY (Leave blank)	2. REPORT DATE 6 August 2001	3. REPORT TYPE AND DATES COVERED Final Report

4. TITLE AND SUBTITLE An Efficient All-Movable Fin Design for Military Aircraft	5. FUNDING NUMBERS F61775-00-WE047
6. AUTHOR(S) Professor Jonathan E Cooper	

7. PERFORMING ORGANIZATION NAME(S) AND ADDRESS(ES) University of Manchester Oxford Road Manchester M13 9PL United Kingdom	8. PERFORMING ORGANIZATION REPORT NUMBER N/A

9. SPONSORING/MONITORING AGENCY NAME(S) AND ADDRESS(ES) EOARD PSC 802 BOX 14 FPO 09499-0200	10. SPONSORING/MONITORING AGENCY REPORT NUMBER SPC 00-4047

11. SUPPLEMENTARY NOTES

12a. DISTRIBUTION/AVAILABILITY STATEMENT Approved for public release; distribution is unlimited.	12b. DISTRIBUTION CODE A

13. ABSTRACT (Maximum 200 words)

This report results from a contract tasking University of Manchester as follows: A generic all-movable vertical tail will be designed (at the conceptual design level) with conventional and with active flexible technologies. The weight, performance and observable benefits of such designs will then be determined relative to the conventional design. The work will examine a range of different parameters including: Mach number - both sub and supersonic speeds, attachment position, yaw stiffness.

The optimisation will be carried out using either the LaGrange code, which is already available at the University of Manchester, or the ASTROS code. A Finite Element model for a generic fin is available which was used in the DASA LaGrange optimisation code. This model was modified previously for the USAF-ASTROS optimisation code. Part of the outcome of this work will be defining the best approach to use such multidisciplinary design and optimization codes to achieve an optimal aeroelastic design.

14. SUBJECT TERMS EOARD, Aero-Structure Interface, Fin Buffeting		15. NUMBER OF PAGES 38
		16. PRICE CODE N/A

17. SECURITY CLASSIFICATION OF REPORT UNCLASSIFIED	18. SECURITY CLASSIFICATION OF THIS PAGE UNCLASSIFIED	19. SECURITY CLASSIFICATION OF ABSTRACT UNCLASSIFIED	20. LIMITATION OF ABSTRACT UL

NSN 7540-01-280-5500

Standard Form 298 (Rev. 2-89)
Prescribed by ANSI Std. 239-18
298-102

FINAL REPORT

AN EFFICIENT ALL-MOVABLE FIN DESIGN FOR MILTARY AIRCRAFT

EOARD CONTRACT F61775-00-WE047

Prof. J. E. Cooper

School of Engineering,
University of Manchester,
Oxford Road, Manchester, M13 9PL, UK

6th August 2001.

SUMMARY

This is the final report describing the work undertaken for EOARD contract F61775-00-WE047 on "An Efficient All-Movable Fin Design for Military Aircraft". The initial part of this study was devoted to investigating the use of the Lagrange Multi-Disciplinary Optimisation code for the aeroelastic optimisation of a generic conventional aircraft fin. Emphasis was placed upon improving the effectiveness characteristics whilst maintaining the strength, aeroelastic stability parameters and also minimising the mass. The second part of the work consisted of a feasibility study into the preliminary design of an all-movable fin. The effects on the aeroelastic behaviour, in particular the fin efficiency, through changes in the attachment position and stiffness were investigated. It was found that both the actuator stiffness and position has a significant effect upon the aeroelastic characteristics, more so than can be achieved solely through variation of structural composite lay-up of a more conventional fixed fin. The all-movable fin design allows significant improvement in the fin efficiency, although this can only be maintained throughout the entire flight envelope with a corresponding reduction in the flutter speed.

CONTENTS

1. INTRODUCTION

The vertical fins of high-speed aircraft suffer from reduced stability and control effectiveness at high dynamic pressures due to aeroelastic effects. A conventional design ensures an adequate tail performance by having a large high aspect ratio fin that consequently needs a stiff and heavy structure. As these large fins are prone to suffering from buffet, the chances of fatigue problems occurring are high. The consequent size and structural requirements lead to further weight, drag and radar cross section penalties.

Until relatively recently, aeroelastic deformation has been considered undesirable. The elastic structural deflections were minimised using a large stiff structure in order to reduce undesirable aeroelastic phenomena. With the development of Multi-Disciplinary Design Optimisation (MDO) methods, the opportunity has arisen to be able to use these elastic deflections to enhance the aerodynamic performance. It is hoped that large weight savings and/or performance improvements will be obtained by using the advantages of flexibility. However, it is necessary to approach the problem in a multi-disciplinary manner in order to satisfy all the aeroelastic constraints (e.g. control reversal, control effectiveness, flutter, divergence and vibration response) otherwise an optimal design cannot be achieved due to the conflicting demands of different disciplines.

The approach of enhancing the aerodynamic performance through the use of the structure's flexibility has been termed Active Flexible Technology (Flick & Love, Pendleton(1998,2000), Schwiger & Krammer). Essentially, this term describes a multi-disciplinary approach that integrates aerodynamics, controls and structures in order to maximise air vehicle performance. This was first described extensively in (Shirk et al. (1984)) and some preliminary analytical studies on an aircraft fin are presented in (Schwiger & Krammer, Tischler et al). Although active flexible technology is currently being developed for aircraft lifting surfaces, it is likely that different optimal solutions will be found when MDO technology is applied to the design of fins due to the contrasting design requirements between the various surfaces. In some cases, the smaller size requirement could remove the necessity for multiple fin surfaces.

An improved fin design would lead to a decrease in tail size and structural weight whilst meeting, or exceeding, all tail performance and observable goals. A further option to fin design is to use an all-movable fin. Here the fin is attached via a single attachment. It is likely that it would be desirable to design the attachment such that it has a variable stiffness, however, the design of such a device to do this is beyond the scope of this work.

The aeroelastic behaviour of simple wings can be explained in terms of the relative location of three important axes a) aerodynamic axis, b) elastic axis and c) mass cg axis. The aerodynamic axis is the loci of aerodynamic centres along the wing span. Similarly, the elastic and mass cg axes are the loci of shear centres and mass cgs of the wing sections. For simple, high aspect ratio, unswept wing with constant cross-section, the elastic axis can be computed easily. These computations can be extended, in an approximate sense, to moderately swept and variable section wings made of isotropic materials. However, the definition of the elastic axis is unclear when applied to low aspect ratio, highly swept wings made of non-isotropic materials. The aerodynamic axis is also difficult to define in the case of severe wing twist. The mass cg axis, on

4

the other hand, is easy to compute although it has no role in explaining the static aeroelastic behaviour. The relative location of these three axes affects the aeroelastic response of the lifting surfaces. The results from the first part of this study are discussed in terms of the relative locations of the various axes. In essence, the optimisation procedures are changing the axes locations, enabling the aeroelastic response to be tailored for improved performance of the lifting surface.

In this work, a generic aircraft fin structure was optimised in order to illustrate the multi-disciplinary approach. The objective was to demonstrate increased effectiveness at high speeds whilst forfilling the constraints of strength and flutter and also minimising the mass. Design parameters that are considered include the CFC lay-up orientation, the skin thickness and the position and stiffness of the attachment points. The second part of the work investigates the effect of varying the attachment stiffness and position on the aeroelastic performance of an all-moving fin.

2.   A GENERIC AIRCRAFT FIN

A typical vertical tail of a fighter was selected for this design study.   A number of other investigators have used various versions of this configuration as a benchmark to test new concepts in the emerging multidisciplinary approach to design (Tishler, Venkayya & Sensburg)

For high speeds, the vertical tail is sized to give a certain minimum value of the directional static stability derivative. For low speed the rudder power unit must be adequate to hold a sideslip of $\beta=11.5^0$ at the approach speed for a cross wind landing.   It also must cover the one engine out case. This low speed requirement may reduce the possibility to cut the fin span and area commensurate with the high-speed design cases

The fin structure is shown in Figure 1. The surface area is 5.46 m^2 and the leading edge sweep angle is 45^0. The fin can be separated into three parts as the fin box, fin tip and rudder. The fin box is built up with six ribs, four spars and symmetric composite skins. The fin tip consists of three ribs, five spars and quasi- isotropic glass fibre skins. The rudder is built up of two spars and six ribs with symmetric composite skins. The fin box has one shear pick-up in the front and one bending attachment at the rear, with the third attachment being located in between. Three hinges couple the fin box to the rudder.
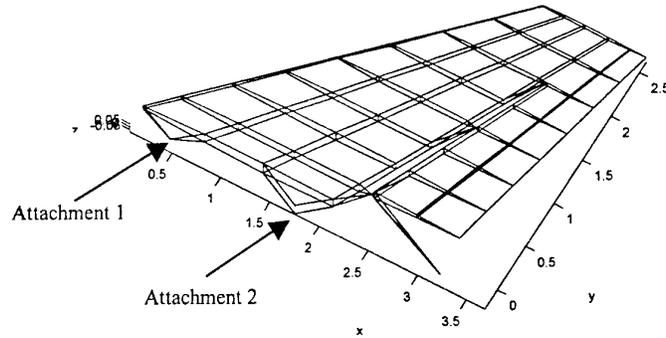
Figure 1 Fin Model

Four materials were used, Carbon Fibre Composite (CFC), Glass Fibre Composite (GFC), Aluminium and Titanium, as follows:

1. Fin Box Skin – Eight layer CFC laminate
2. Rudder Skin – Six layer CFC laminate
3. Tip Skin – Quasi Isotropic GFC
4. Fin Box Rear Spar – Four layer CFC laminate
5. Rudder Main Spar – Four layer CFC laminate
6. Remaining Spars – Aluminium
7. Rudder Start Rib – Titanium
8. Rudder End Ribs – Titanium
9. Remaining Ribs – Isotropic CFC
10. Connecting Rods – Aluminium
11. Fin Attachments – Titanium

3.   AEROELASTIC MODELLING

The static aeroelastic response of a structure subjected to external forces can be described by the simple equation

$$KU = P(U) \qquad (1)$$

where K is the stiffness matrix of the structure, and U is the vector of displacements, defined in reference to the structure's degrees of freedom. The left-hand side of the equation represents the elastic forces in equilibrium with the aerodynamic forces on the right hand side. Note that as the forces due to the airflow are related to the deformation of the structure P is expressed as a

function of **U**. The static aeroelastic case infers that there are no inertia forces on the right hand side of the equation.

An approximate form of **P(U)** can be written as

$$\mathbf{P(U)} = q\mathbf{AU} + q\mathbf{A}^{\alpha}\alpha + q\mathbf{A}^{\delta}\delta \qquad (2)$$

where q is the dynamic pressure, $\dfrac{\rho V^2}{2}$, ρ is the air density and V is the free stream velocity. **A** is the aerodynamic influence coefficient matrix with respect to the displacement degrees of freedom. $\mathbf{A}^{\alpha}$ and $\mathbf{A}^{\delta}$ are due to the lifting surface and the control surface angles of attack. α is the initial angle of attack and δ is the control surface displacement.

The case of static divergence of the lifting surface is represented by

$$[\mathbf{K} - q\mathbf{A}]\mathbf{U} = 0 \qquad (3)$$

The solution of this complex eigenvalue problem (corresponding to the lowest real positive value) yields both the divergence dynamic pressure and the divergence velocity.

The lift effectiveness is another important static aeroelastic parameter, and it is defined as the ratio of the lift of the flexible surface compared to that achieved for a rigid surface. It can be written as

$$LE = \frac{C_{LF}}{C_{LR}} = \frac{q\mathbf{h}^T\mathbf{A}^{\alpha}\alpha + q\mathbf{h}^T\mathbf{AU}}{\mathbf{h}^T\mathbf{A}^{\alpha}\alpha} \qquad (4)$$

where C_{LF} is the flexible lift and C_{LR} is its rigid counterpart, and where **h** is a vector consisting of the aerodynamic panel lengths. Solving Equation 3 for **U** with $\delta = 0$ and substituting into Equation 4 gives the lift effectiveness equation

$$LE = \frac{\mathbf{h}^T\left[\mathbf{I} + q\mathbf{A}[\mathbf{K} - q\mathbf{A}]^{-1}\right]\mathbf{A}^{\alpha}\alpha}{\mathbf{h}^T\mathbf{A}\alpha} \qquad (5)$$

Similar expressions can be derived for control surface effectiveness as well as the critical flutter velocity.

4.   MBB-LAGRANGE

MBB-Lagrange is the multidisciplinary analysis and optimisation system for the design of aircraft structures. There are two linked parts consisting of structural analysis and optimisation models. The structural analysis section provides the essential structural aspects. With the use of finite element analysis, static and dynamic analysis of complicated structures can be accomplished. The static disciplines consist of displacement and strength computations, and the

dynamic disciplines are modal analysis, frequency response and transient response analysis. Aeroelastic analysis is also included in the system. The static aeroelastic elements compute the control effectiveness and divergence speeds of lifting surfaces. Flutter analysis is provided for by the dynamic aeroelastic analysis part.

In the optimisation model, a number of gradient-based optimisation methods e.g. sequential linear and quadratic programming, and sensitivity analysis strategies are available. Design problems can be set for either a sizing optimisation or weight minimisation. Design parameters can be cross-sectional area, plate thickness and ply-orientation of composite structures. The constraints imposed upon the optimisation are the disciplines described above in the analysis section.

5.   DESIGN CONDITIONS

The optimisation problem for the design studies is posed as:

Minimise an objective function $f(\mathbf{x})$

subject to structural constraints
$$g_i(\mathbf{x}) \le g_{0,i}: i = 1,\ldots,m$$

and bound constraints

$$\mathbf{x}^l \le \mathbf{x} \le \mathbf{x}^u$$

where $\mathbf{x}$ is a vector of design variable size n and $\mathbf{x}^l$ and $\mathbf{x}^u$ are lower and upper bounds of $\mathbf{x}$ respectively.

Sequential linear programming (SLP) was employed to solve the problem. The procedure is to start with an initial solution $\mathbf{x}^0$ consisting of the design variables (skin thickness and the fibre orientations of fin box skins and rudder skins). The solution is then improved iteratively toward the optimum solution. The objective function was the fin mass. The minimum bound of the thickness is imposed at 0.25 mm while the upper limit is set to be 10.0 mm. The lower and upper bounds of the fibre orientations are 0° and 180° respectively. The constraints of the fin are as follows:

- Static constraints
  Aerodynamic forces due to five different flight conditions of the fin under both subsonic and supersonic flows are chosen as static load cases. The strain constraints for CFC composite skins are:
      The allowable tension and compression strains in the fibre direction are 0.003 and -0.003 respectively.
      The allowable tension and compression strains in the transverse direction are 0.003 and -0.003 respectively.
      The allowable shear strain is 0.003.

For the displacement constraints, the displacement of the end rib of the fin tip is imposed at −350 mm lower limit and 350 mm upper limit.

- Control effectiveness constraints
  Two control effectiveness were defined - the effectiveness due to the fin having lift incidence and the effectiveness due to deflection of the rudder at the 1.8 Mach case with steady aerodynamics.

- Flutter constraint
  The minimum allowable flutter speed of the fin at 1.2 Mach number is set as a constraint function.

6.   DESIGN CASES

Three design cases were considered to study the possibility of improving the fin efficiency. The study cases were as follows:

- OPT1: optimisation of the fin with various attachment positions
  The positions of the front and middle attachment points are varied in the x-direction leading to 16 various attachment aspects. With the 16 different structures, the optimisation is operated so that the minimum weight of each structure is obtained. The attachment points are given in Table 1. The constraints, fin efficiency, rudder efficiency and flutter speed, are set at 1.0, 0.565, and 530 m/s respectively.

- OPT2: optimisation of the fin with various flutter speed and fin efficiency constraints.
  The task is to improve the fin efficiency whilst minimising the weight and meeting strain constraints. Table 2 shows the various fin efficiency and flutter speed values. The rudder efficiency was taken at 0.565 for each design case considered here.

	1	2	3	4
Attachment1	450.0	616.7	783.3	950.0
Attachment2	1750	1933.3	2116.7	2300.0

Table 1 Positions of Attachments in x-direction for OPT1(mm)

	1	2	3	4
Fin Efficiency	1.2	1.3	1.4	1.5
Flutter (m/s)	500.0	515.0	530.0	545.0

Table 2 Flutter and Fin-efficiency Constraints for OPT2

9

7.   OPTIMISATION RESULTS

As there are a number of fins with different attachment aspects, for simple explanation the fin with attachment points at [450.0, 1750.0], [616.7,1933.3] and [950.0,2300.0] will be defined as the 11–ATT fin, 22–ATT fin and 44–ATT fin respectively. The optimum results of the fin due to varying the attachment points (OPT1) are illustrated in Figure 2. It is shown that the attachment points [450.0,1750.0] gives the minimum fin weight comparing to the optimum results of the others.

Figure 2 Minimum Weight vs. Attachment Positions of OPT1

The simple explanation is to find an equivalent beam representing the fin that would be located at the elastic axis. The shear centre of each cross section is achieved by establishing the point in the plane of cross section at which a normal shear load can be applied without twisting the section.

By applying the moment at the fin tip, the deflection of nodal points is obtained. The deflection throughout the fin surface can then be estimated by using surface spline interpolation (Harder and Desmarais). The elastic axis of the fin follows the points on the surface that have zero deflection.

Figure 3 shows the elastic axis location of the optimum 11–ATT fin. From the figure the elastic axis is located behind the aerodynamic axis of supersonic Ma 1.8 which can be said that any initial angle of attack can be increased leading to high fin efficiency. The elastic axis of the optimum 44–ATT fin is illustrated in Figure 4.

Figure 3 Elastic and Aerodynamic Axes of the Optimum Fin with 11-Attachment
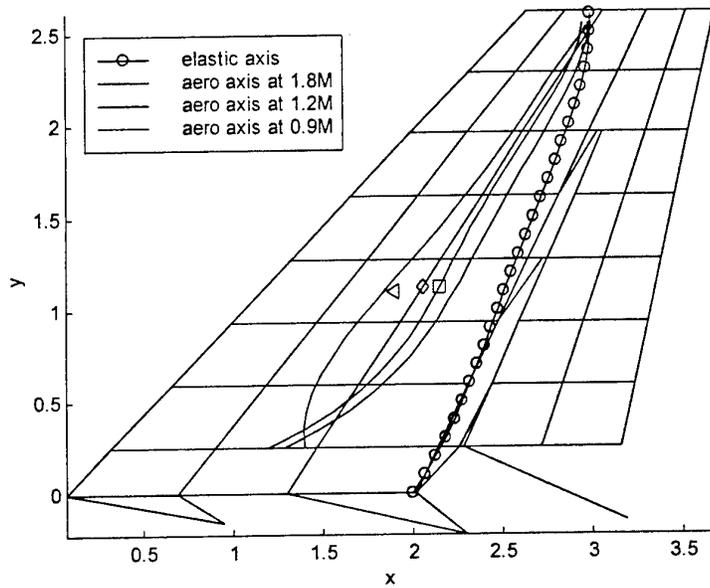
Figure 4 Elastic and Aerodynamic Axes of the Optimum the Fin with 44-Attachment

The elastic axis moves backward from the 1.8 Ma aerodynamic axis more than the previous axis. That means using this attachment is advantageous in term of improving fin efficiency. Nevertheless, as the flutter is analysed at Ma 1.2, moving an elastic axis too far way from the aerodynamic axis at Ma 1.2, flutter speed can be reduced as the pitching moment on the fin is increased. Therefore, it can be said that, with all of the attachment points, the optimisation operation can drive the elastic axes backward behind the 1.8 Ma aerodynamic axis which means the fin efficiency can be improved reaching or even exceeding the constraint point 1.0. The more backward attachment gives the higher fin efficiency. Then the real attention will be flutter constraint. The elastic axis of the 11–ATT fin is closer to the 1.2 Ma aerodynamic axis than the elastic axes of the rests. The more forward attachment will give the more increasing flutter speed. As a result, with the constraints of OPT1, the 11–ATT fin has the lighter optimum weight than the other fins.
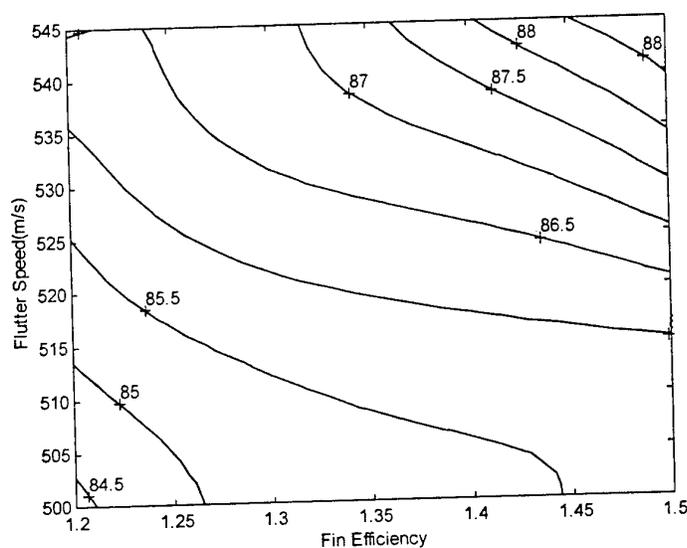
Figure 5 Minimum Mass VS Flutter and Efficiency Constraints of the Fin with 11-attachment

For the OPT2 case study, the fin efficiency and flutter constraints are varied such that improving aeroelastic characteristics of the fin and minimising the fin mass simultaneously. Figure 5 shows the optimum results of the 11–ATT fin.

The optimum results of the 44–ATT fin are shown in figure 6 while the optimum results of the 22–ATT fin are shown in figure 7. At the extreme point of constraints (545 m/s flutter speed, and 1.5 fin efficiency), the optimum weight of the 11–ATT fin, 44–ATT fin, and 22–ATT fin are 88.84 kg, 108.04 kg and 84.71 kg respectively.
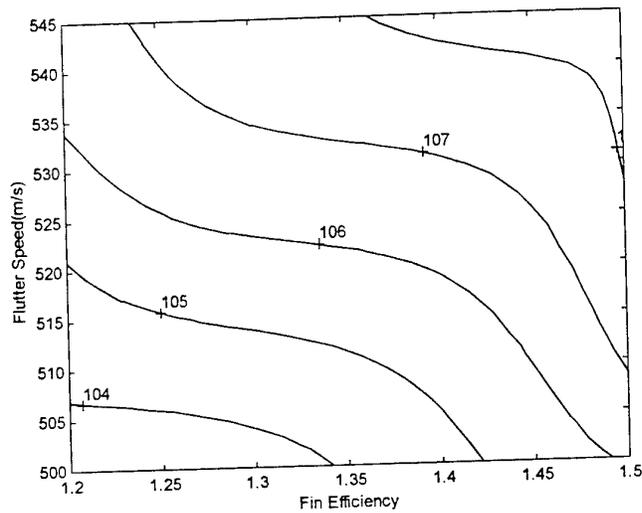
Figure 6 Minimum Mass VS Flutter and Efficiency Constraints of the Fin with 44-attachment
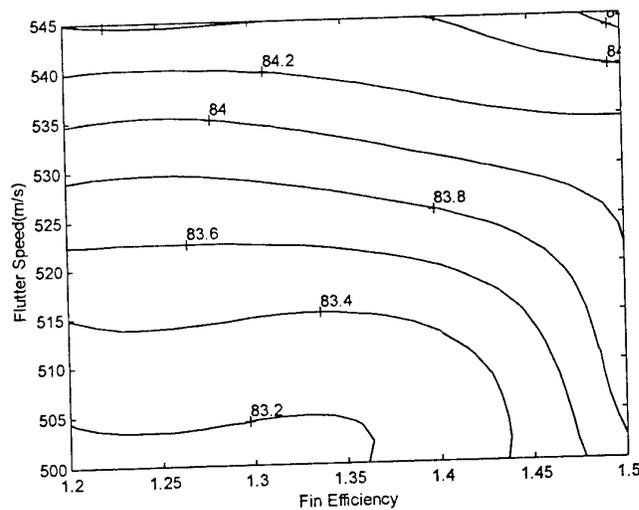
Figure 7 Minimum Mass VS Flutter and Efficiency Constraints of the Fin with 22-attachment

The elastic axes of the entire optimum fins are shown in Figures 8-10. Figure 8 shows the elastic axis of the optimum 11–ATT fin. As the elastic axis is located close to the 1.2 Ma aerodynamic axis, the fin can be improved to reach the flutter constraint but it is difficult to improve the fin efficiency. Figure 9 shows the elastic axis of the optimum 44–ATT fin. The fin can ease to exceed 1.5 fin-efficiency but it will have some difficulties to reach the flutter speed of 545 m/s. The elastic axis of the optimum 22–ATT fin, which is in between the other two attachments, is shown in Figure 10. The axis is located in between the previous two axes. This attachment can

13

be said to be is the trade-off between the [430,1750] and [950,2300] attachments. It is slightly difference between the optimum mass of the 22–ATT fin and 11–ATT fin. However, as the improvement of fin efficiency is more required, the 22-ATT fin will be advantageous if the higher fin-efficiency constraint is assigned.
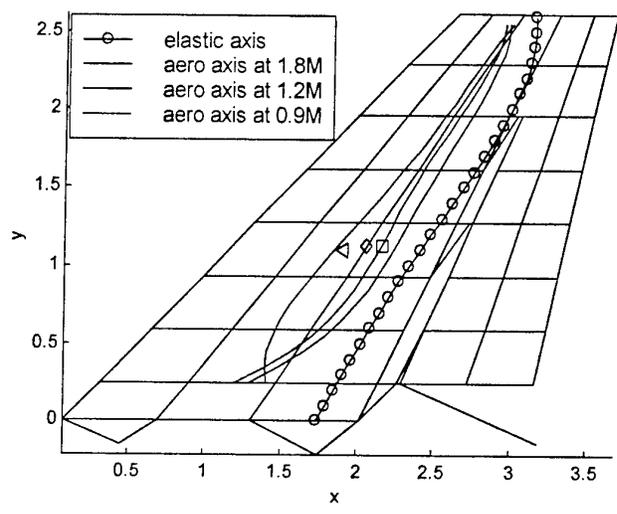
Figure 8 Elastic and Aerodynamic Axes of the Optimum 11-ATT Fin at 545 m/s Flutter and 1.5 Fin-efficiency
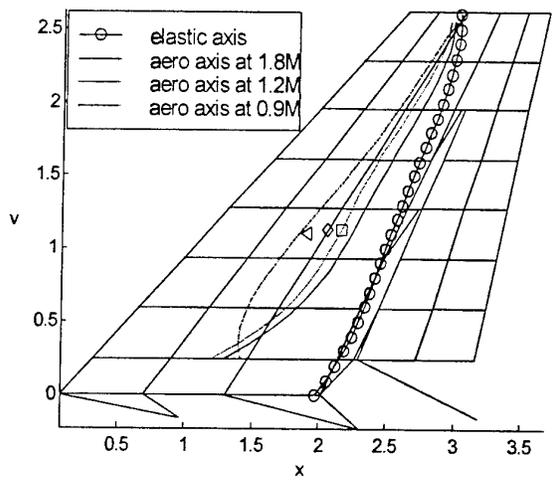
Figure 9 Elastic and Aerodynamic Axes of the Optimum 44-ATT Fin at 545 m/s Flutter and 1.5 Fin-efficiency
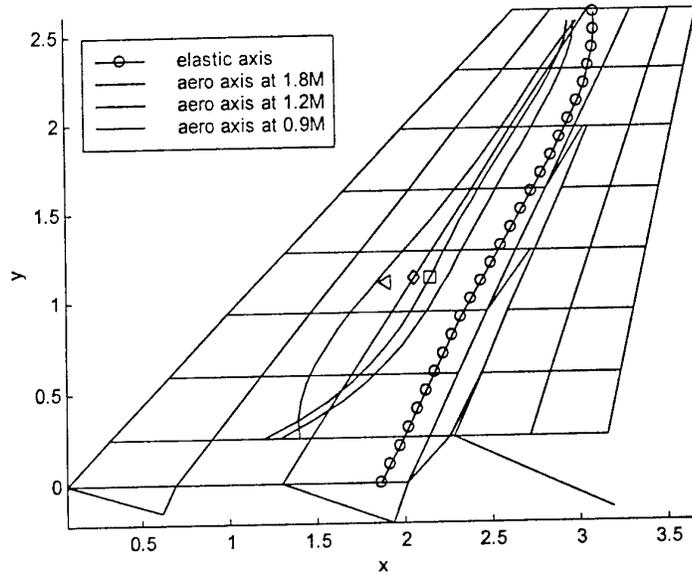
Figure 10 Elastic and Aerodynamic Axes of the Optimum 22-ATT Fin at 545 m/s Flutter and 1.5 Fin-efficiency

The results show that it is possible to achieve much higher fin efficiency values with little increase in mass whilst still achieving flutter speed and other structural constraints. Consequently, it is possible to use structural flexibility as a benefit for aeroelastic design, rather than something that has to be suppressed.

8. ALL-MOVING FIN

As a preliminary investigation into possibilities of using an all moving fin to gain a design advantage aeroelastically, several of the above cases were changed so that there was only a single attachment, as shown in Figure 11. Flutter speeds, modal characteristics and fin efficiencies were calculated for a range of different Mach numbers, attachment positions and attachment stiffnesses. A selection of results is shown here for the structure obtained with the 22-ATT fin. It was found that the fin structure had less bearing upon the characteristics than the attachment itself. Figures 12-18 show the various attachment positions whilst figure19 shows how the single attachment was modeled.

The variation of the natural frequencies of the first 5 modes (the modes that conribute to the aeroelastic behaviour) with varying torsional stiffness is illustrated in figures 20 to 26. These results are shown in a different manner for each individual mode in figures 27 to 30 and the corresponding mode shapes are plotted in figures 31 to 35.

Of particular interest in this work was the effectiveness of the fin for varying attachment conditions. Figures 36 to 42 show how the efficiency varies with torsional stiffness at the various attachment points, whereas figures 43 to 49 show how the efficiency changes with torsional stiffness for different Mach numbers. Finally, figue 50 shows how the flutter speed changes with different attachment positions and stiffnesses. All of these results for the all-movable fin are tabulated in tables 3 to 9.
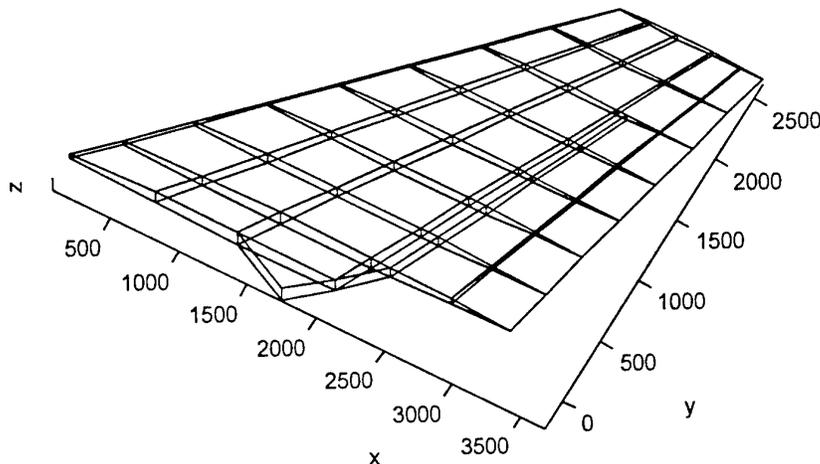
Figure 11 All-moveable Fin

16
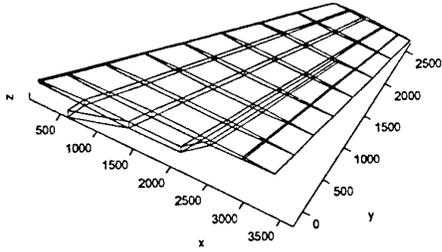
Figure 12. 600mm Attachment
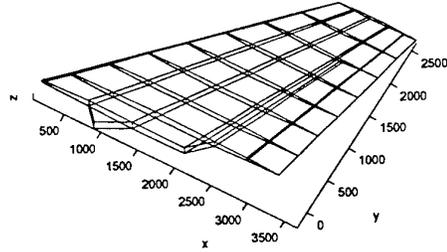
Figure 13. 900mm Attachment
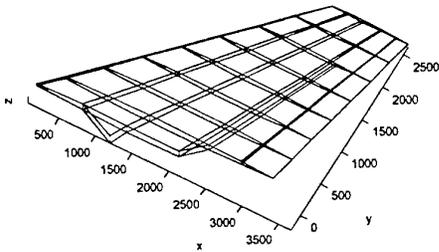
Figure 14. 1200mm Attachment
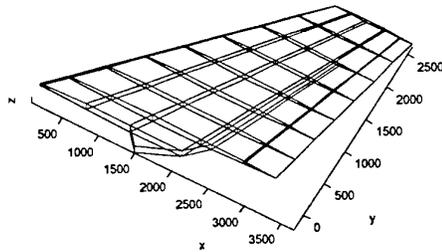
Figure 15. 1500mm Attachment

Figure 16. 1750mm Attachment
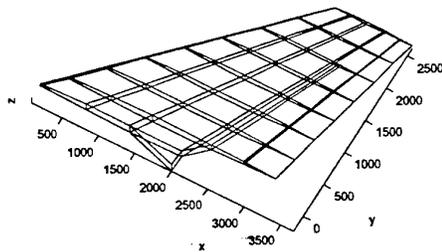
Figure 17. 2000mm Attachment

17
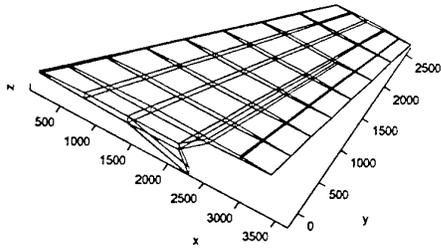
Figure 18. 2300mm Attachment
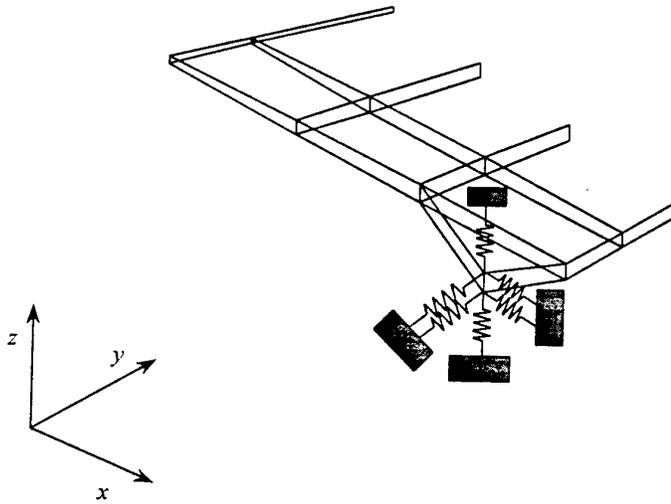
Figure 19. Attachment Stiffness
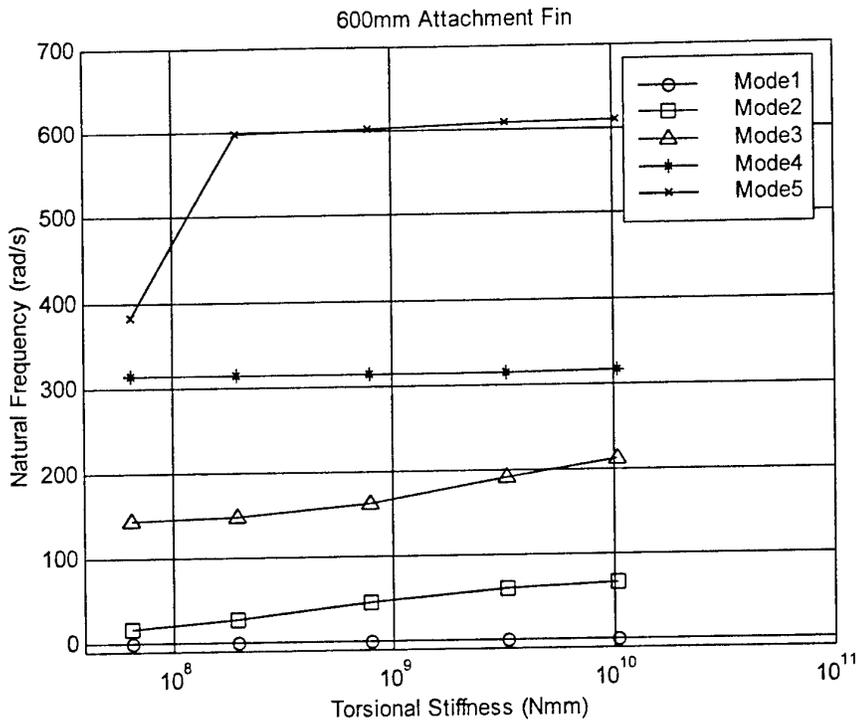
Figure 20 Attachment Torsional Stiffness VS Natural Frequency of 600mm-Att Fin
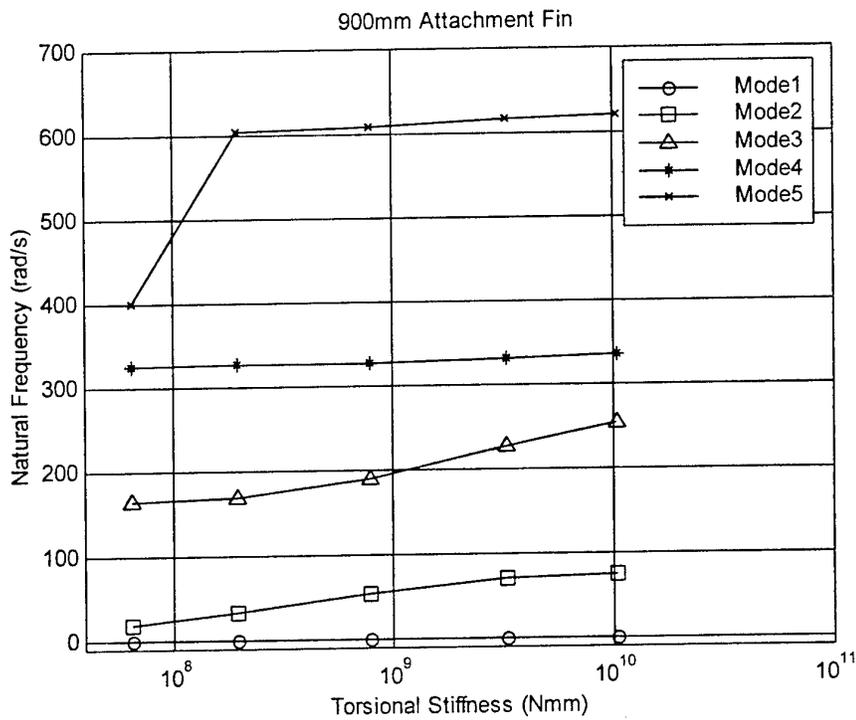
Figure 21. Attachment Torsional Stiffness VS Natural Frequency of 900mm-Att Fin

19
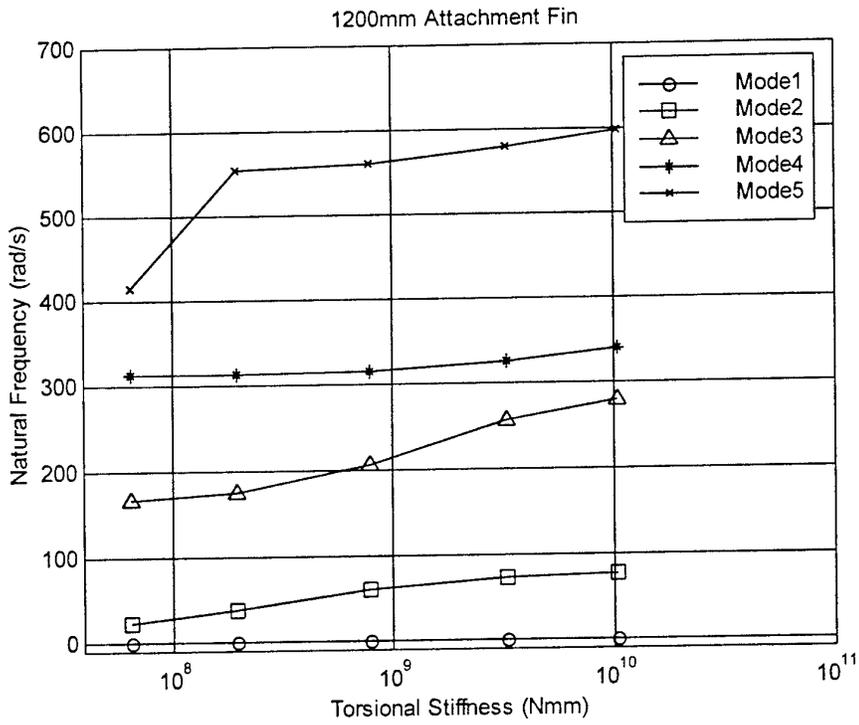
Figure 22. Attachment Torsional Stiffness VS Natural Frequency of 1200mm-Att Fin
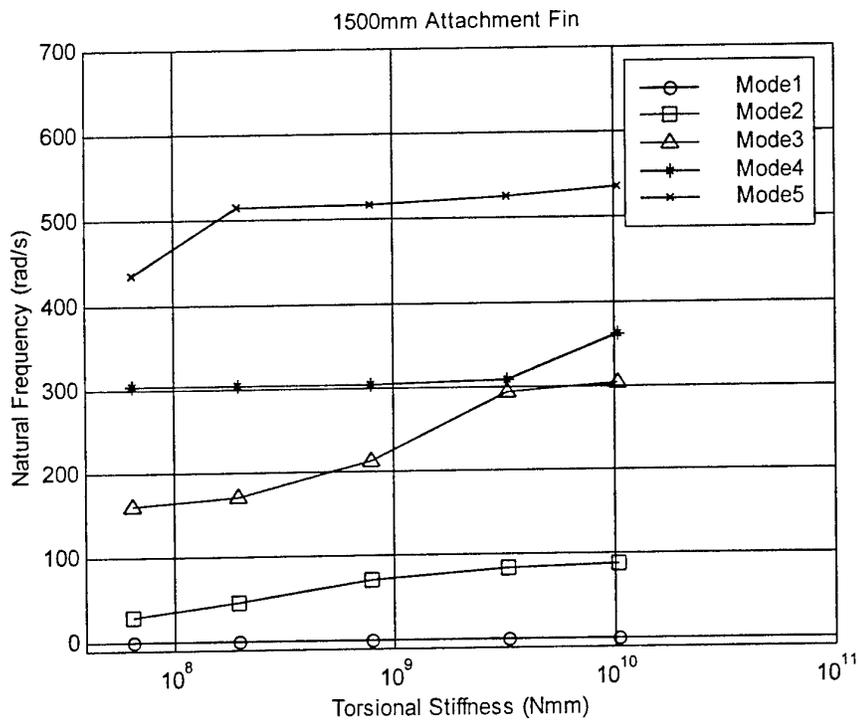
Figure 23 Attachment Torsional Stiffness VS Natural Frequency of 1500mm-Att Fin
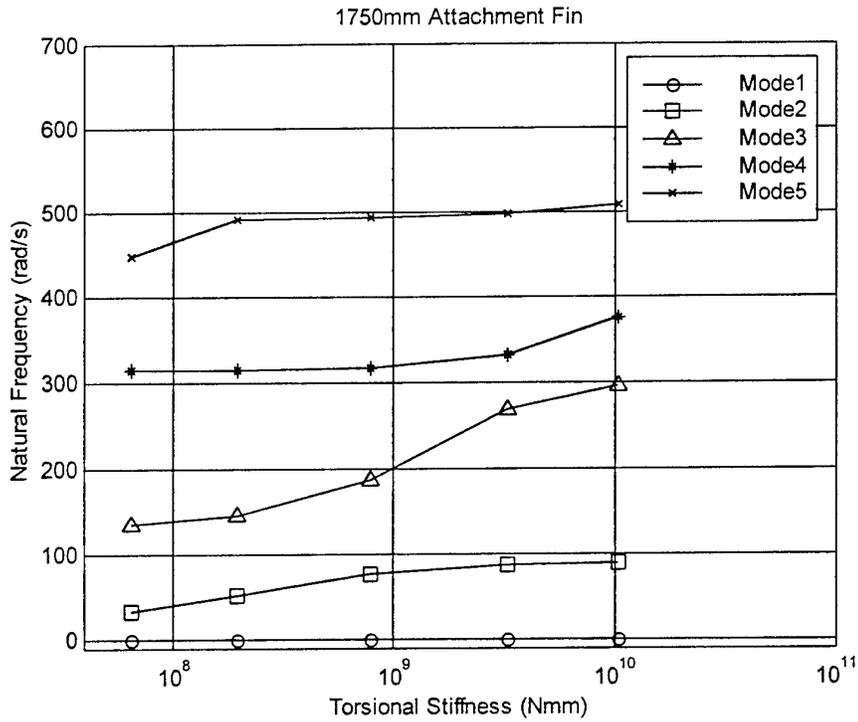
Figure 24. Attachment Torsional Stiffness VS Natural Frequency of 1750mm-Att Fin
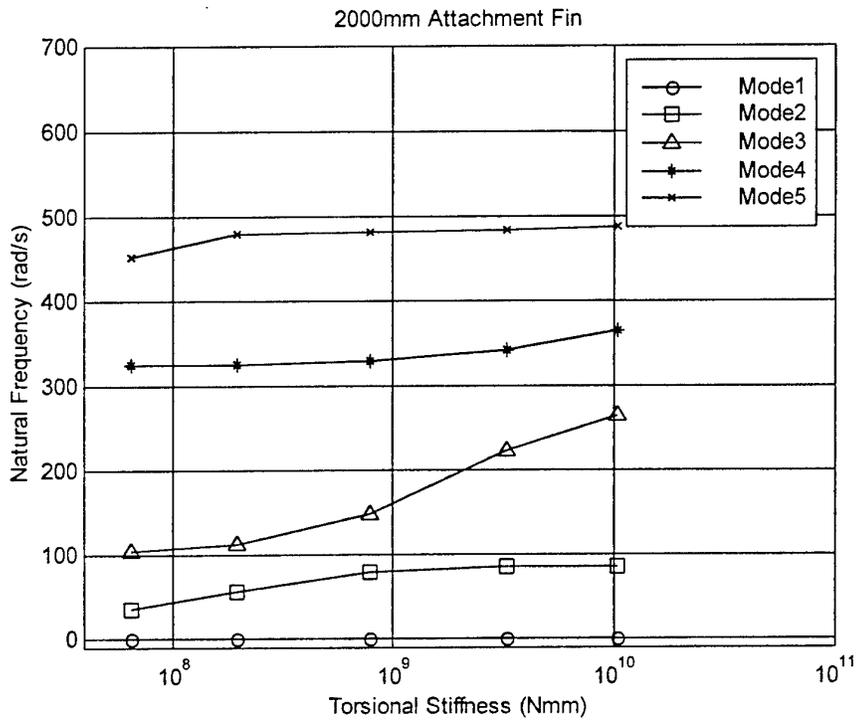
Figure 25. Attachment Torsional Stiffness VS Natural Frequency of 2000mm-Att Fin
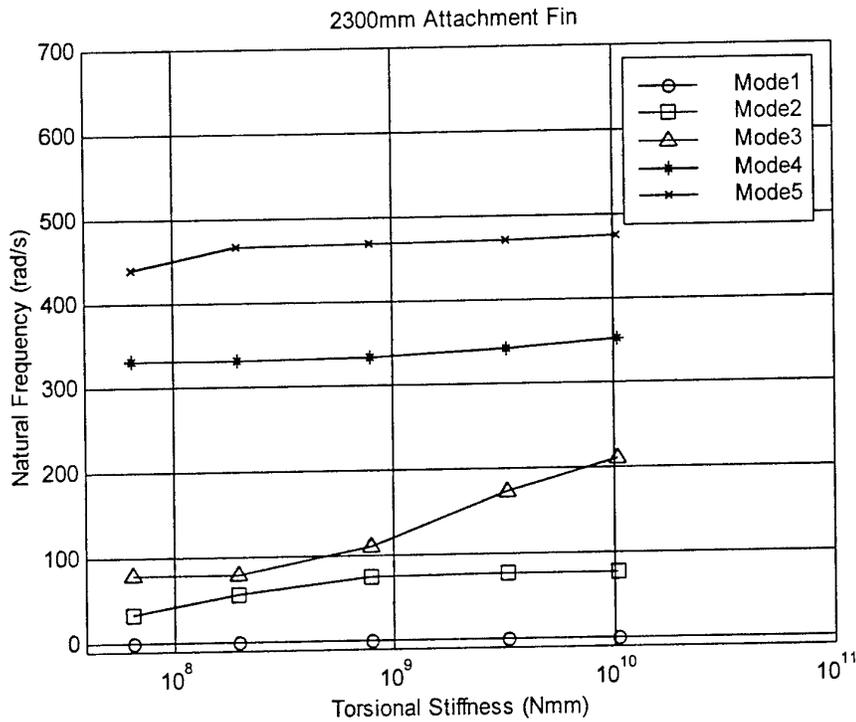
Figure 26. Attachment Torsional Stiffness VS Natural Frequency of 2300mm-Att Fin
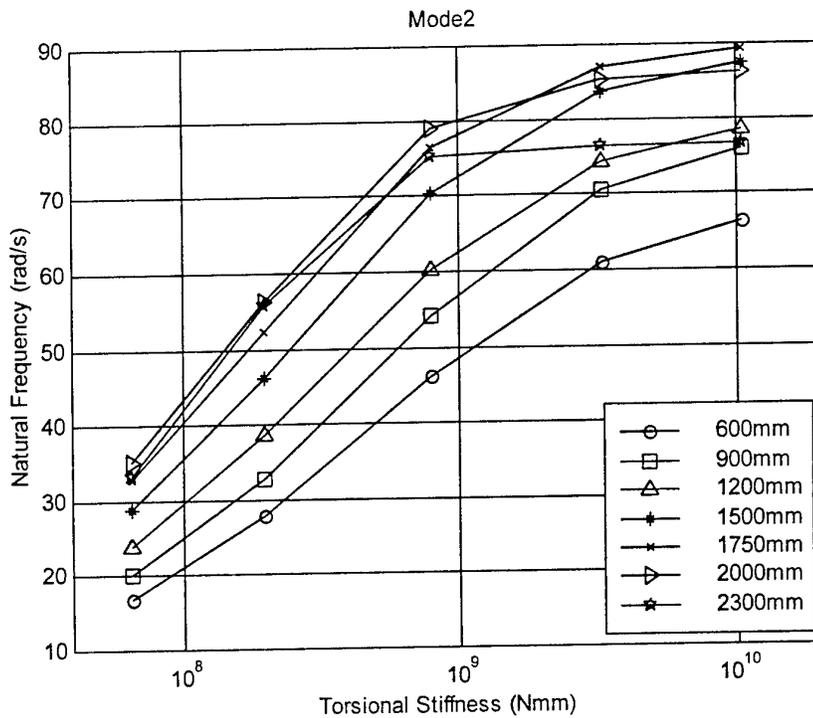
Figure 27. Attachment Torsional Stiffness VS Natural Frequency at Mode 2
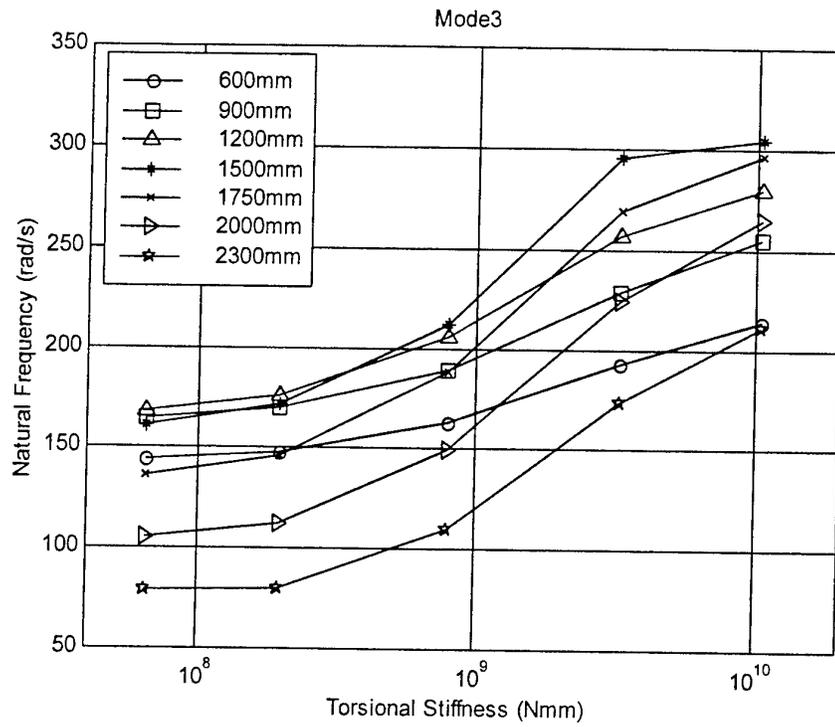
Figure 28. Attachment Torsional Stiffness VS Natural Frequency at Mode 3
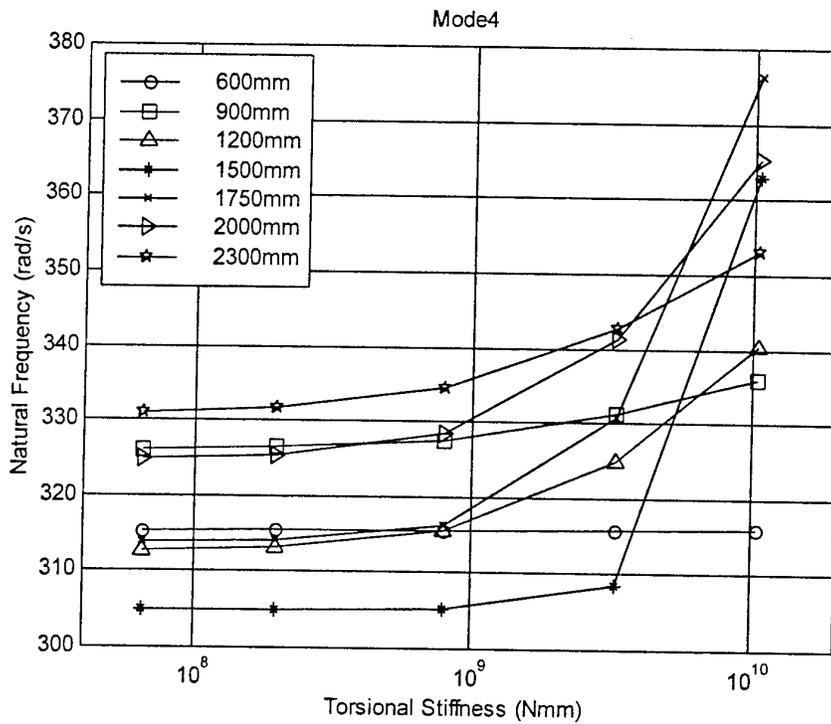
Figure 29 Attachment Torsional Stiffness VS Natural Frequency at Mode 4

23
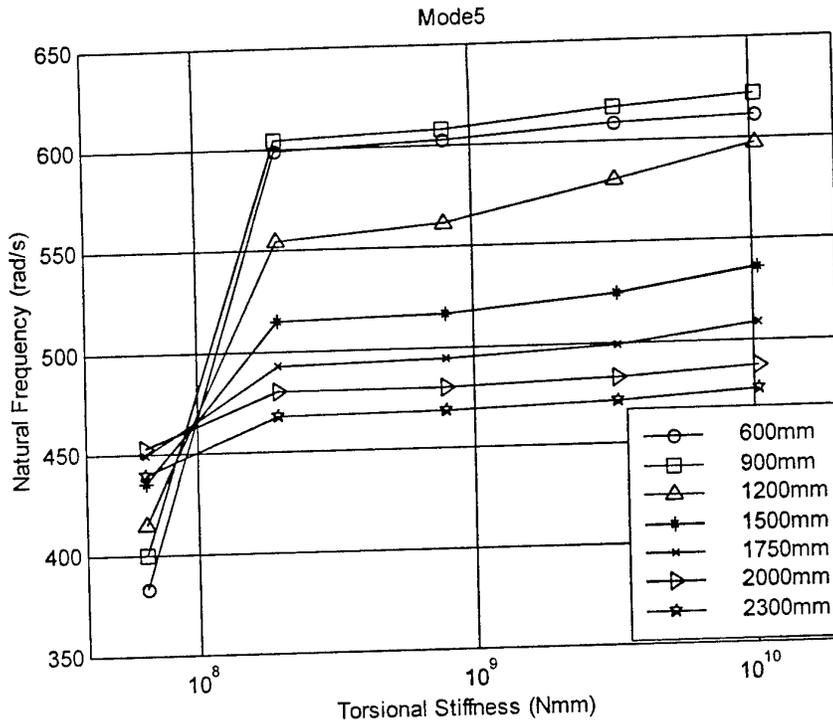
Mode5

Figure 30 Attachment Torsional Stiffness VS Natural Frequency at Mode 5

Mode1
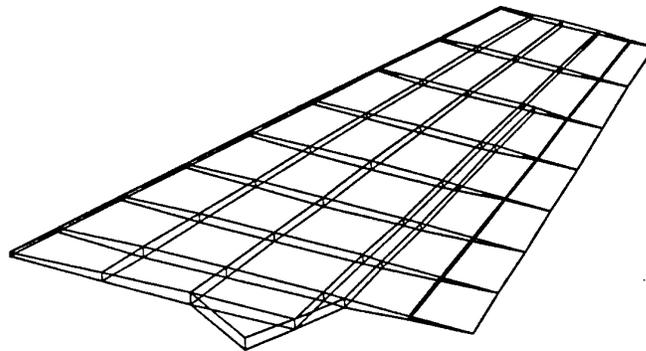
Figure 31. Fin Natural Mode 1

Mode2
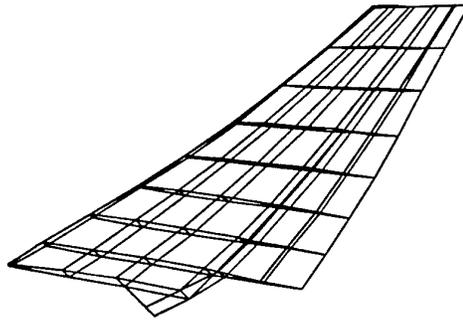
Figure 32. Fin Natural Mode 2

Mode3
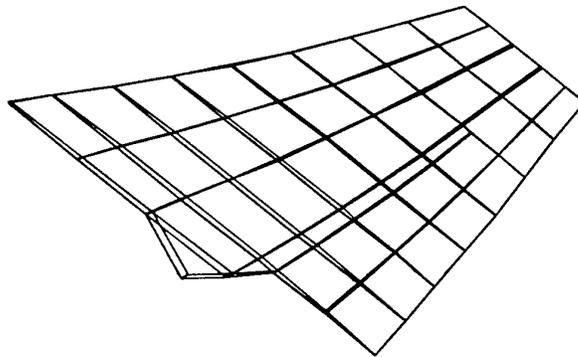
Figure 33. Fin Natural Mode 3

Mode4
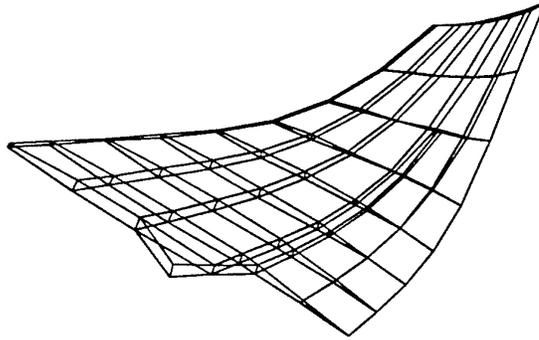
Figure 34. Fin Natural Mode 4

Mode5
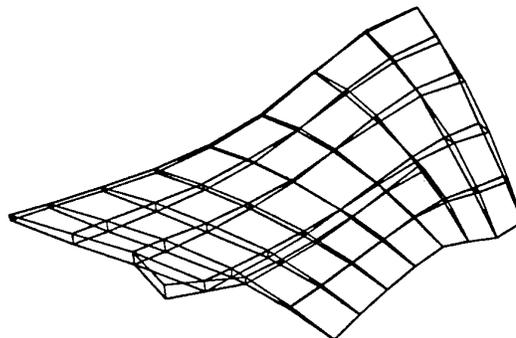
Figure 35. Fin Natural Mode 5

26
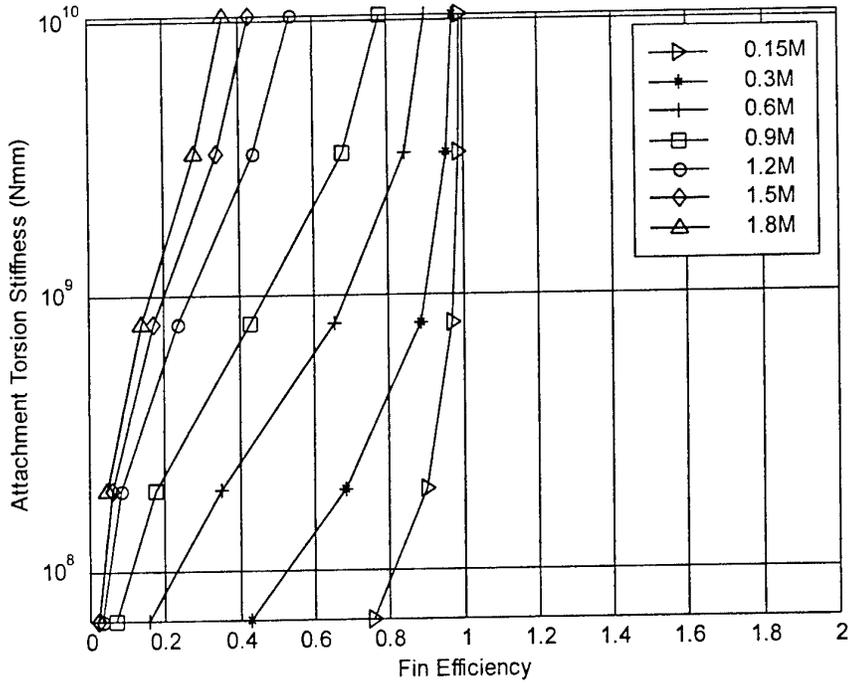
Figure 36. Fin Efficiency VS Torsional Stiffness for 600mm Attachment Point
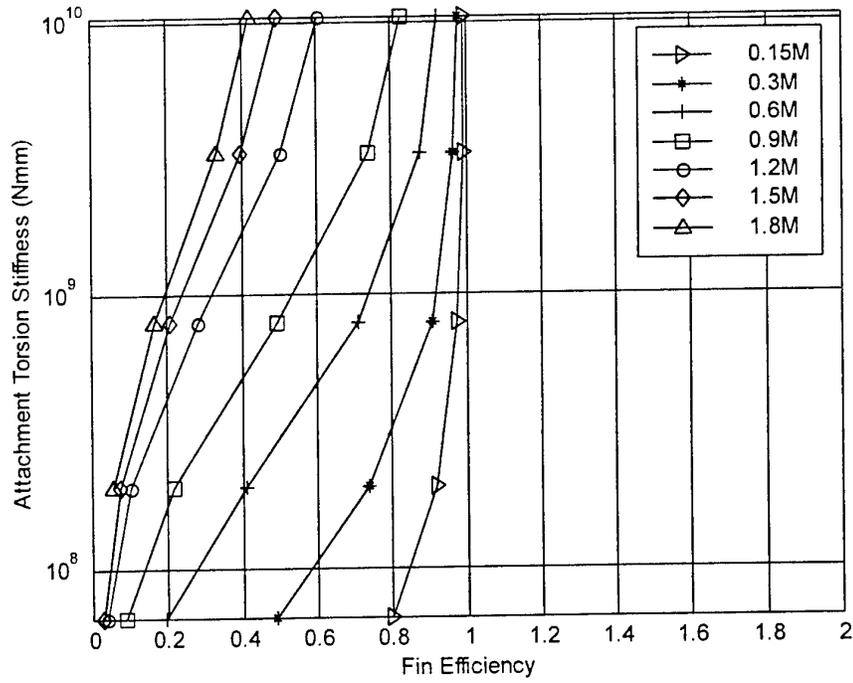
Figure 37. Fin Efficiency VS Torsional Stiffness for 900mm Attachment Point
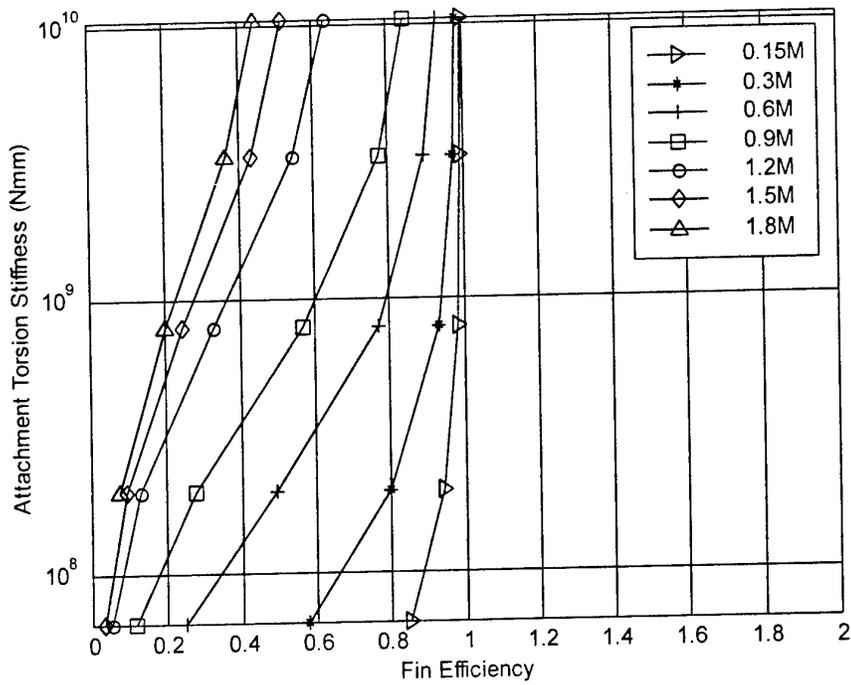
Figure 38. Fin Efficiency VS Torsional Stiffness for 1200mm Attachment Point
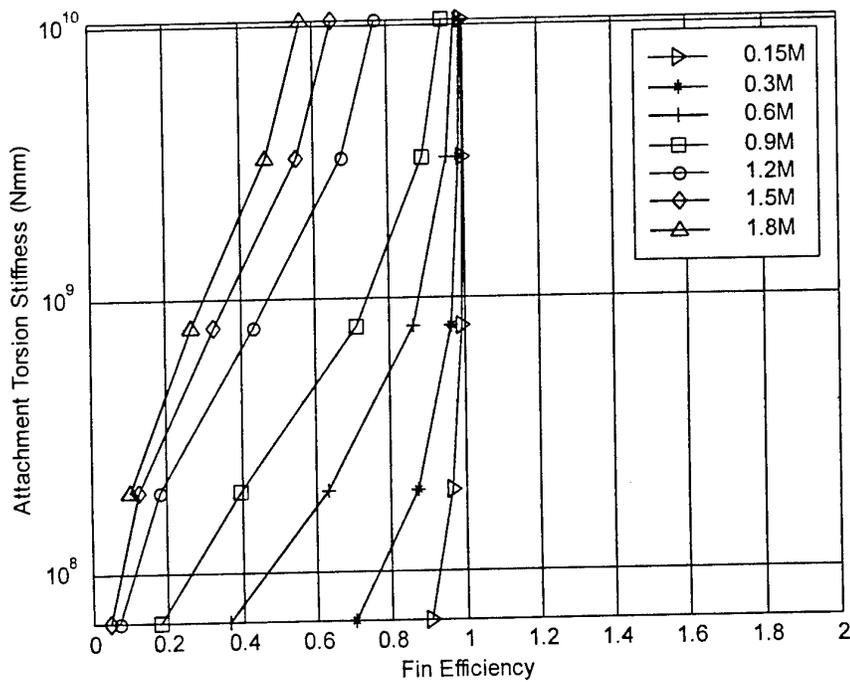
Figure 39. Fin Efficiency VS Torsional Stiffness for 1500mm Attachment Point
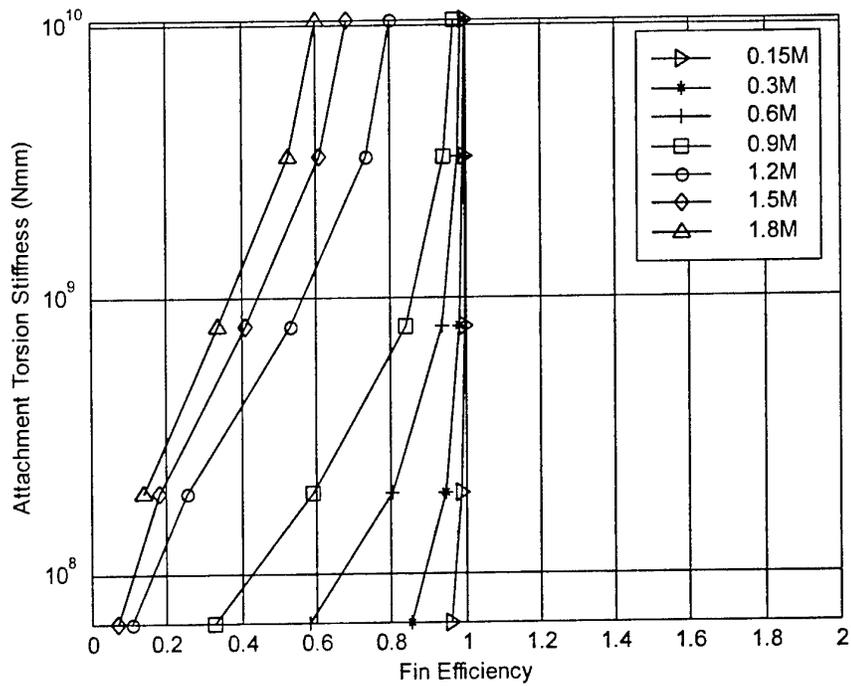
Figure 40. Fin Efficiency VS Torsional Stiffness for 1750mm Attachment Point
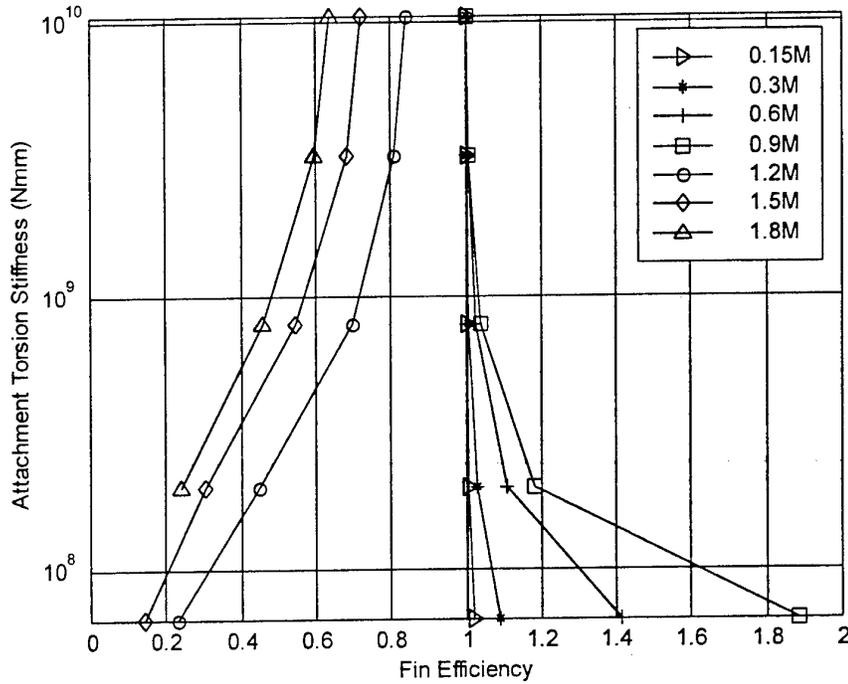
Figure 41. Fin Efficiency VS Torsional Stiffness for 2000mm Attachment Point
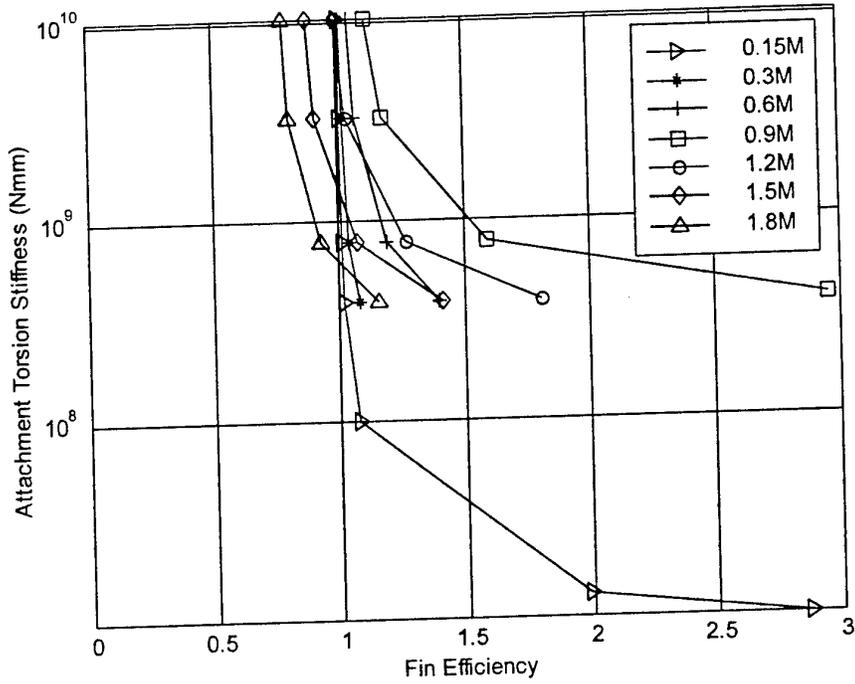
Figure 42. Fin Efficiency VS Torsional Stiffness for 2300mm Attachment Point
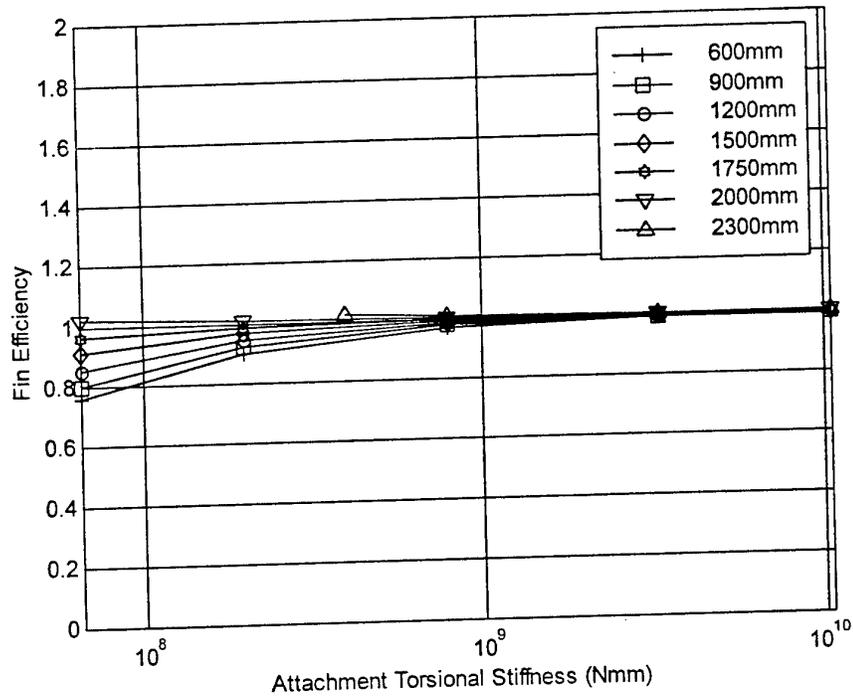
Figure 43. Fin Efficiency VS Torsional Stiffness at 0.15 Ma

30
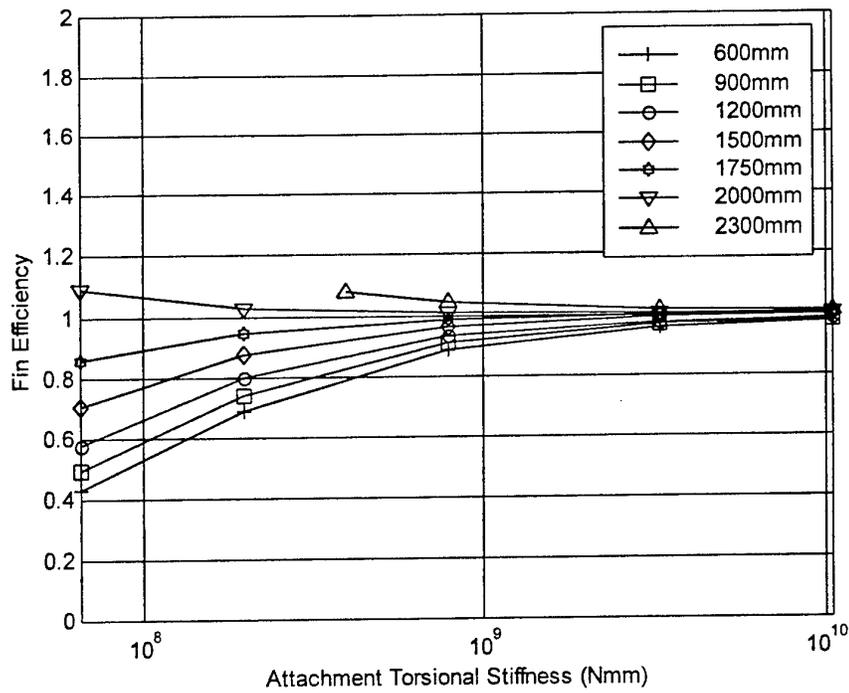
Figure 44. Fin Efficiency VS Torsional Stiffness at 0.3 Ma
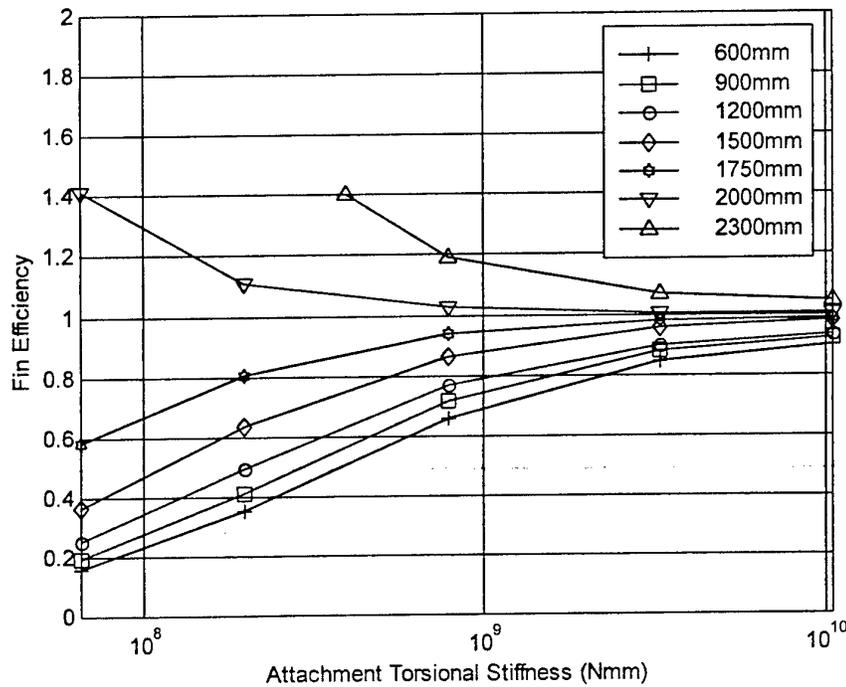
Figure 45. Fin Efficiency VS Torsional Stiffness at 0.6 Ma
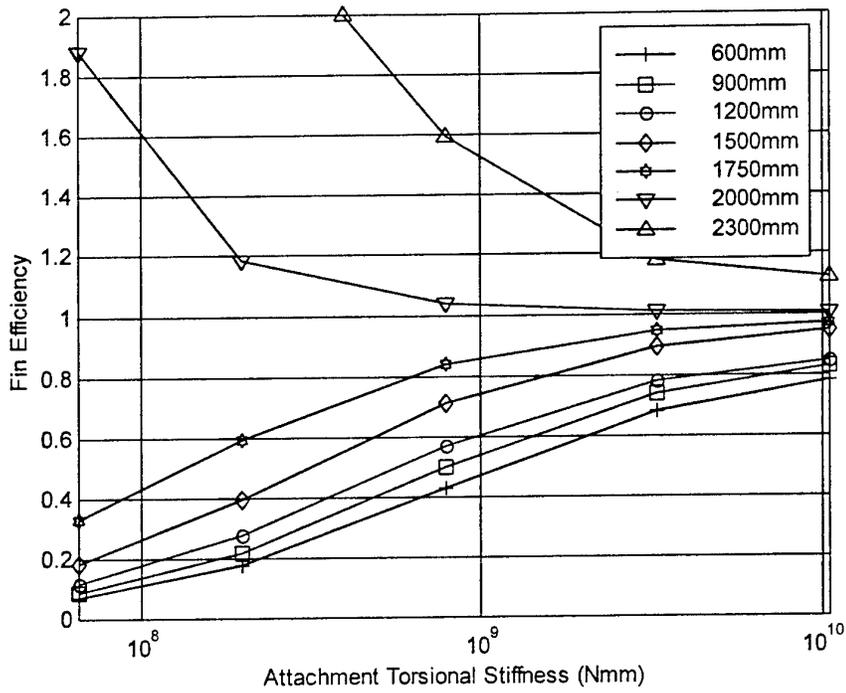
Figure 46. Fin Efficiency VS Torsional Stiffness at 0.9 Ma
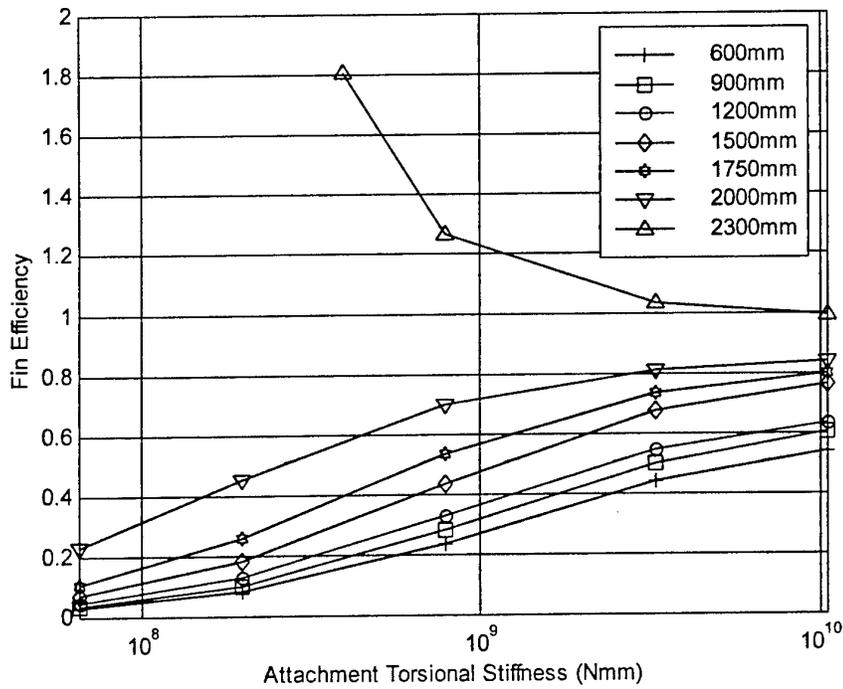
Figure 47. Fin Efficiency VS Torsional Stiffness at 1.2 Ma

32
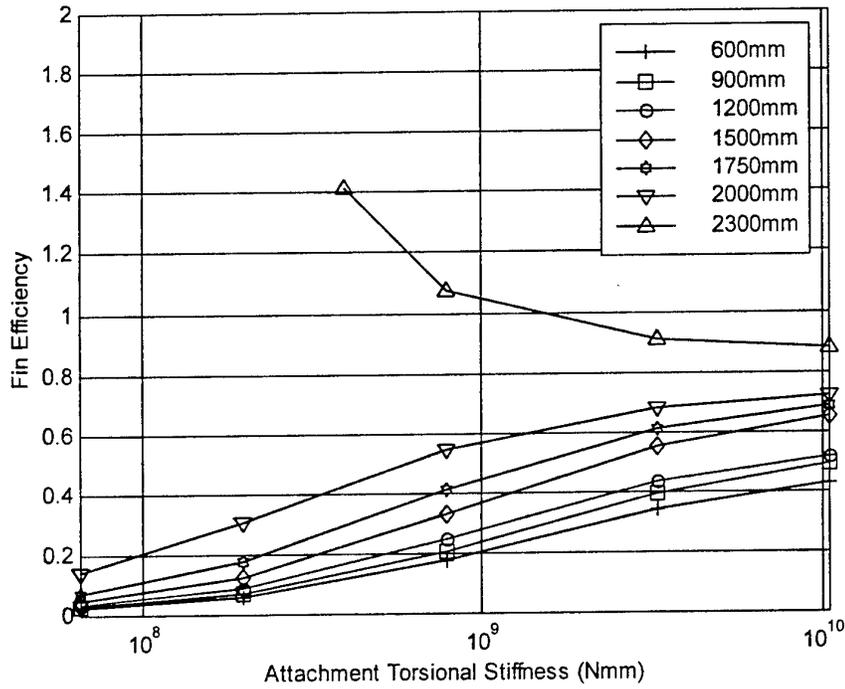
Figure 48. Fin Efficiency VS Torsional Stiffness at 1.5 Ma
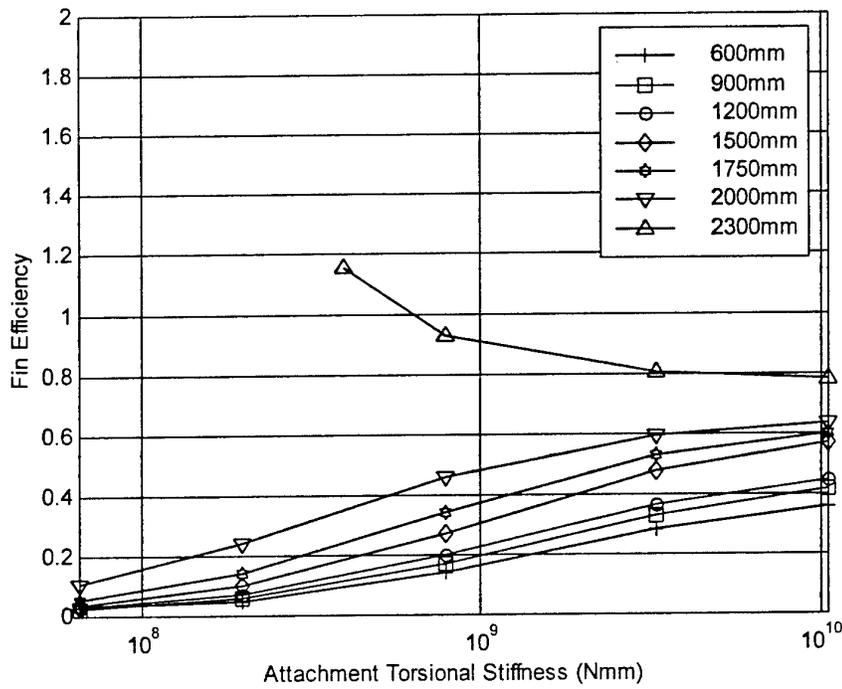
Figure 49. Fin Efficiency VS Torsional Stiffness at 1.8 Ma
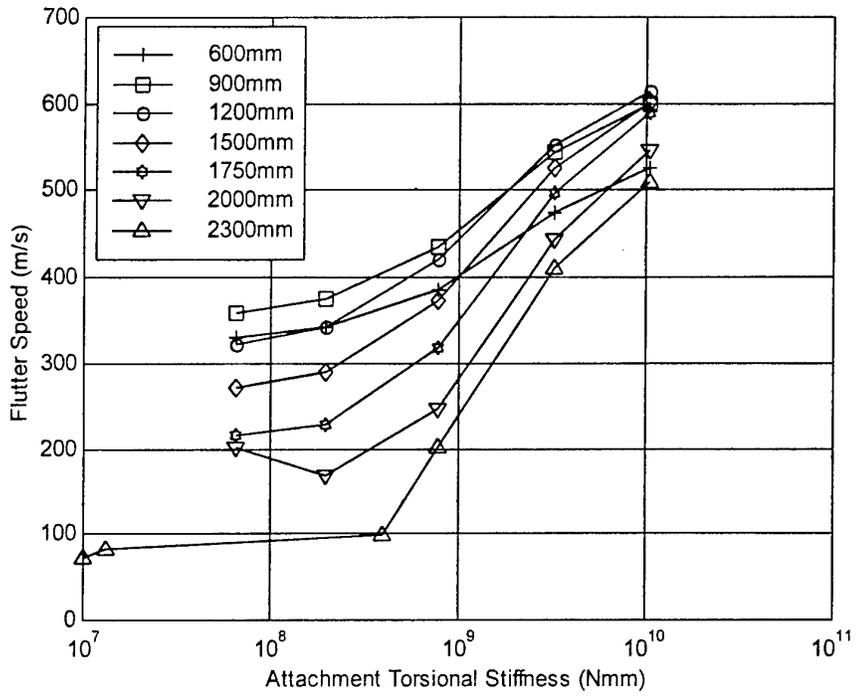
Figure 50. Torsional Stiffness VS Flutter Speed

All-Movable Fin Efficiency

Attachment position	6.561×10^7 (Nmm)	1.968×10^8 (Nmm)	7.873×10^8 (Nmm)	3.2811×10^9 (Nmm)	1.050×10^{10} (Nmm)
600mm	0.7554	0.9001	0.9698	0.9892	0.9935
900mm	0.8001	0.9212	0.9767	0.9918	0.9952
1200mm	0.8495	0.9423	0.9826	0.9933	0.9957
1500mm	0.9076	0.9668	0.9910	0.9973	0.9987
1750mm	0.9607	0.9862	0.9987	0.9987	0.9993
2000mm	1.0208	1.0069	1.0005	1.0005	1.0002
2300mm	1.0181 (3.937×10^8Nmm)		1.0101	1.0047	1.0028

Table 3 All-Movable Fin Efficiency at 0.15 Ma.

Attachment Position	6.561×10^7 (Nmm)	1.968×10^8 (Nmm)	7.873×10^8 (Nmm)	3.2811×10^9 (Nmm)	1.050×10^{10} (Nmm)
600mm	0.4277	0.6855	0.8858	0.9566	0.9735
900mm	0.4918	0.7387	0.9101	0.9669	0.9802
1200mm	0.5769	0.7978	0.9316	0.9730	0.9825
1500mm	0.7030	0.8751	0.9636	0.9889	0.9946
1750mm	0.8539	0.9448	0.9842	0.9947	0.9970
2000mm	1.0889	1.0280	1.0070	1.0017	1.0006
2300mm	1.0784 (3.937×10^8Nmm)		1.0426	1.0169	1.0115

Table 4 All-Movable Fin Efficiency at 0.30 Ma.

Attachment Position	6.561×10^7 (Nmm)	1.968×10^8 (Nmm)	7.873×10^8 (Nmm)	3.2811×10^9 (Nmm)	1.050×10^{10} (Nmm)
600mm	0.1558	0.3498	0.6563	0.8435	0.8992
900mm	0.1926	0.4106	0.7133	0.8771	0.9232
1200mm	0.2511	0.4922	0.7696	0.8978	0.9314
1500mm	0.3660	0.6306	0.8651	0.9551	0.9771
1750mm	0.5806	0.8020	0.9358	0.9771	0.9866
2000mm	1.4157	1.1078	1.0242	1.0050	1.0010
2300mm	1.3993 (3.937×10^8Nmm)		1.1903	1.0689	1.0458

Table 5 All-Movable Fin Efficiency at 0.60 Ma.

Attachment Position	6.561×10^7 (Nmm)	1.968×10^8 (Nmm)	7.873×10^8 (Nmm)	3.2811×10^9 (Nmm)	1.050×10^{10} (Nmm)
600mm	0.0683	0.1759	0.4308	0.6808	0.7790
900mm	0.0861	0.2158	0.4961	0.7395	0.8276
1200mm	0.1160	0.2753	0.5680	0.7775	0.8452
1500mm	0.1809	0.3953	0.7119	0.8931	0.9454
1750mm	0.3292	0.5906	0.8412	0.9426	0.9679
2000mm	1.8833	1.1845	1.0397	1.0085	1.0019
2300mm	2.9501 (3.937×10^8Nmm)		1.5937	1.1809	1.1181

Table 6 All-Movable Fin Efficiency at 0.90 Ma.

Attachment Position	6.561×10^7 (Nmm)	1.968×10^8 (Nmm)	7.873×10^8 (Nmm)	3.2811×10^9 (Nmm)	1.050×10^{10} (Nmm)
600mm	0.0309	0.0833	0.2353	0.4381	0.5390
900mm	0.0378	0.1018	0.2796	0.5014	0.6057
1200mm	0.0492	0.1289	0.3293	0.5435	0.6328
1500mm	0.0701	0.1794	0.4323	0.6727	0.7651
1750mm	0.1075	0.2561	0.5327	0.7335	0.7989
2000mm	0.2315	0.4499	0.6969	0.8096	0.8390
2300mm	1.8092 (3.937×10^8Nmm)		1.2670	1.0319	0.9920

Table 7 All-Movable Fin Efficiency at 1.20 Ma.

Attachment Position	6.561×10^7 (Nmm)	1.968×10^8 (Nmm)	7.873×10^8 (Nmm)	3.2811×10^9 (Nmm)	1.050×10^{10} (Nmm)
600mm	0.0251	0.0589	0.1731	0.3405	0.4311
900mm	0.0271	0.0718	0.2069	0.3956	0.4932
1200mm	0.0339	0.0906	0.2453	0.4326	0.5186
1500mm	0.0476	0.1256	0.3275	0.5527	0.6498
1750mm	0.0711	0.1780	0.4093	0.6105	0.6835
2000mm	0.1413	0.3067	0.5471	0.6829	0.7218
2300mm	1.4157 (3.937×10^8Nmm)		1.0743	0.9079	0.8784

Table 8 All-Movable Fin Efficiency at 1.50 Ma.

Attachment Position	6.561×10^7 (Nmm)	1.968×10^8 (Nmm)	7.873×10^8 (Nmm)	3.2811×10^9 (Nmm)	1.050×10^{10} (Nmm)
600mm	0.0299	0.0468	0.1396	0.2810	0.3602
900mm	0.0248	0.0571	0.1679	0.3305	0.4185
1200mm	0.0272	0.0720	0.2001	0.3643	0.4433
1500mm	0.0372	0.0994	0.2686	0.4727	0.5661
1750mm	0.0548	0.1403	0.3383	0.5268	0.5993
2000mm	0.1054	0.2391	0.4568	0.5938	0.6351
2300mm	1.1575 (3.937×10^8Nmm)		0.9268	0.8048	0.7824

Table 9 All-Movable Fin Efficiency at 1.80 Ma.

9. DISCUSSION OF ALL-MOVING FIN RESULTS

Examination of figures 20 – 26 show that the characteristics of the modes involved do not vary much of the range of attachments considered, although there are some changes in the ordering at the higher stiffnesses for mode 2 – 4 whilst these changes in order occurs at the lower torsional stiffnesses for mode 5. Analysis of the modal characteristics showed that changing the structural lay-up orientation did not have any significant influence and this aspect is consequently not included in the rest of this report.

Figures 36 – 42 show how the fin efficency varies with torsional stiffness for the various attachment positions. For positions 600mm to 1750mm a decrease in the stiffness results in a decrease in the fin efficiency, and this effect is excentuated for higher Mach numbers. However, for the 2000mm attachment, a decrease in the torsional stiffness leads to efficiencies greater than one for the sub-sonic speeds. There is still a reduction in efficiency for the supersonic cases. Figure 42 shows that if the attachment is placed even further back, then it is possible to achieve above unity efficiency values for all the speeds cases.

Figures 43 – 49 show the same information in a different form. It is clear the advantages of placing the attachment further back. However, figure 50 shows the trade-off that must be made with the above advantage. The further back that the attachment is placed, the lower the flutter speed becomes.

10. CONCLUSIONS

The use of the Lagrange Aeroelastic Optimisation package has been demonstrated upon a conventional generic fin. It was shown how the structure could be optimised to improved the aeroelastic efficiency whilst still maintaining its previous performance.

An initial study into the performance of a generic all-moving fin with variable attachment position and stiffness was also performed. The results demonstrated that it is possible to achieve a significant improvement in fin efficiencies by placing the attachment further back. However, this effect is countered by a lowering of the flutter speed. It is felt that the best way to approach this design would be to have an attachment that is capable of having a variable stiffness. If a fully variable stiffness were not feasible, then a design with two stiffnesses, one for low and the other for high speeds would be desirable.

11. FUTURE WORK

- Wind-tunnel investigation to verify the aeroelastic characteristics observed in this study of a generic all-moving fin with varying attachement stiffness and position.
- Investigation into the design issues relating to high and low speed flight. It is envisaged that a variable stiffness actuator may be required
- Investigation into the feasibility of designing an attachment for a full-size fin
- Investigation into the feasibility of different approaches for adaptive attachments for the all-moving fin

12. REFERENCES

Flick, P. & Love, M. (1999) 'The Impact of Active Aeroelastic Wing Technology on Conceptual Aircraft Design'. AVT Panel Meeting. Ottawa.

Harder, R. L. and Desmarais, R. N.(1972), 'Interpolation Using Surface Splines', J. Aircraft, vol. 1, no 2, 1972, pp. 189-191.

Pendleton, E., Bessette, D., Field, P., Miller, G. & Griffen, K. (1998), ' The Active Aeroelastic Wing Flight Research Program' 39th SDM Conference

Pendleton, E.(2000), 'Back to the Future How Active Aeroelastic Wings are a Return to Aviation's Beginnings and a Small Step to Future Bird-like Wings',RTO-SMP Panel Meeting.

Shirk, M.H., Hertz, T.J. & Weisshaar, T.A. (1984) 'A Survey of Aeroelastic Tailoring Theory, Practice, Promise' AIAA Paper 84-0982-CP 25th SDM Conference.

Schwiger, D. & Krammer, J., (1999) 'Active Aeroelastic Aircraft and its Impact on Structure and Flight Control System Design'. AVT Panel Meeting. Ottawa.

Tischler, V. A., Venkayya, V. B. and Sensburg, O. (2000), 'Aeroelastic Tailoring of Empennage Structures', AIAA-2000-1326. 41st SDM Conference, Atlanta.